

Effect of Microwaves on Superconductors for Kinetic Inductance Detection and Parametric Amplification

A.V. Semenov^{1,2,*}, I.A. Devyatov^{3,2,†}, M.P. Westig⁴ and T.M. Klapwijk^{4,1}

¹*Physics Department, Moscow State University of Education, 1 Malaya Pirogovskaya st., Moscow 119992, Russia*

²*Moscow Institute of Physics and Technology, Dolgoprudny, Moscow 141700, Russia*

³*Lomonosov Moscow State University, Skobeltsyn Institute of Nuclear Physics, 1(2), Leninskie gory, GSP-1, Moscow 119991, Russia*

⁴*Kavli Institute of NanoScience, Faculty of Applied Sciences, Delft University of Technology, Lorentzweg 1, 2628 CJ Delft, Netherlands*



(Received 17 December 2018; revised manuscript received 27 October 2019; accepted 15 January 2020; published 28 February 2020)

We address parametric amplifiers and kinetic inductance detectors, using concepts of the microscopic theory of superconductivity, and focusing on the interaction of microwave radiation with the superconducting condensate. This interaction was identified in recent experiments as the source of the apparent dissipation in microwave superconducting microresonators at low temperatures. Since the evaluation of the performance of practical devices based only on changes in kinetic inductance is not sufficiently informative about the underlying physical processes, we design an experiment with a tunnel measurement of a microwave-driven superconducting wire, in which the tunneling process is not affected by the microwaves. We conclude that such an experiment is feasible with current technology, but is unfortunately difficult to incorporate into standard superconducting resonators optimized for performance in applications. Nevertheless, given the limits of the commonly used phenomenological theories, such an experiment will provide the groundwork for further optimization of the performance.

DOI: [10.1103/PhysRevApplied.13.024079](https://doi.org/10.1103/PhysRevApplied.13.024079)

I. INTRODUCTION

In recent years there has been increased interest in the use of conventional superconductors in the presence of a microwave field, for example in quantum computation [1,2], parametric amplification [3], and astronomical multipixel detection with microwave kinetic inductance sensors [4,5]. The subject is also closely related to efforts to measure the Higgs mode in superconductors [6–9]. The experiments are carried out far below the critical temperature of the superconductor, where few quasiparticles are present and the properties of the response to the microwave field are dominated by the superconducting condensate.

A commonly used assumption about the nonlinear response of a superconductor is summarized by writing the kinetic inductance as

$$L_k(I) \approx L_k(0) \left[1 + \left(\frac{I}{I_*} \right)^2 \right], \quad (1)$$

where I_* is the scale of the nonlinearity and $L_k(0) = \hbar R_n / \pi \Delta$, with being R_n the resistance in the normal state

and Δ the superconducting energy gap. This expression is an adaptation of the standard Ginzburg-Landau analysis of a dc-current-carrying superconductor [10], assuming $I/I_* \ll 1$. The underlying microscopic picture is of a supercurrent carried by Cooper pairs, which at rest have net zero momentum ($\vec{k} \uparrow, -\vec{k} \downarrow$). When a supercurrent flows, all Cooper pairs have a net momentum, \vec{p}_s , or are pairs with $[(\vec{k} + \vec{p}_s) \uparrow, (-\vec{k} + \vec{p}_s) \downarrow]$. The kinetic energy stored in the moving condensate is at the expense of the net condensation energy, which results in a reduced order parameter Ψ , i.e., a reduced energy gap Δ . In order to apply this analysis to the kinetic inductance at high frequencies, ranging from microwave to terahertz frequencies, the time response of the system is important too [11]. For the instantaneous response of the order parameter to a change in the supercurrent, the quantity I_* differs from that for a delayed response, because of the very long relaxation time. Such a time delay has been experimentally observed [10] by applying current pulses with a current larger than the critical current, causing, with indium as the superconductor, a time delay on the order of nanoseconds, in agreement with an energy-relaxation time of 148 ps. Both the Ginzburg-Landau analysis and the analytical expressions for the nonequilibrium response are applicable only close to the critical temperature of the superconductor, T_c . The new

*av.semyonov@mpgu.edu

†Deceased.

applications are at much lower temperatures, where the order parameter is energy dependent, and the response to radiation needs to take into account the change in the density of states (DOS) due to the absorbed radiation. In addition, the microwave frequency needs to be considered in comparison with the characteristic relaxation times.

Experimentally, it was demonstrated by de Visser *et al.* [12] that the resonant frequency of an Al superconducting resonator shifts with increasing microwave power. This shift appears to be analogous to a temperature rise, although the applied frequency ω_0 has a photon energy much lower than the energy gap Δ , which rules out pair breaking by the photon energy. In addition, because the measurements were carried out far below T_c , the density of quasiparticles was very low. Therefore, we study theoretically the nature of a superconducting condensate which oscillates at a frequency ω_0 due to an applied microwave field. It has been demonstrated [13] that a microwave field has a depairing effect on a superconductor, analogous to that of a dc current [14–17], but qualitatively different. The DOS loses its sharp peak at the gap energy, which is comparable to what happens with a dc current, but in addition it acquires features at specific energies $\Delta \pm n\hbar\omega_0$, where Δ is the modulus of the order parameter. These features in the density of states are a manifestation of Floquet states, which are the eigenstates of any quantum system exposed to a periodic field [18]. It was also shown [13] that the DOS develops an exponential-like tail in the subgap region.

The present study is carried out to relate the phenomenological expression in Eq. (1) and the recently observed microscopic properties of a superconductor with an oscillating condensate. On general grounds, we expect that the quadratic dependence will not change, but we would like to be able to calculate the parameters. In addition, a conceptual understanding of the response of a uniform superconductor, such as aluminum, assumed here may provide insight that will help us to understand also the difference from the response of inhomogeneous superconductors such as niobium titanium nitride ((Nb,Ti)N) [19] or granular aluminum (GrAl) [20]. In the present paper, we present additional theoretical results for a realistic case by including inelastic scattering. In addition, we present the design of an experiment which would enable a measurement of the microscopic parameters with a tunnel probe of a superconductor exposed to a microwave field, while at the same time avoiding the possibility that the tunneling process, intended as a passive probe, is affected by the microwave field.

II. ACTION OF MICROWAVES ON THE SUPERCONDUCTING CONDENSATE

In order to go beyond the phenomenological Ginzburg-Landau theory, we need to use the microscopic theory of nonequilibrium superconductivity [21–24]. This allows us

to access the practically relevant regime of $\Delta \gg k_B T$ and includes the fact that the superconducting properties are dependent on the energy. This dependence is very well known from tunneling experiments, but it also enters the response of the superconducting condensate to microwave radiation. We assume a dirty superconductor, i.e., one with an elastic mean free path ℓ much smaller than the BCS coherence length ξ_0 , meaning that we can rely on the Usadel theory [25] for impurity-averaged Green's functions. As shown by Stoof and Nazarov [26] and Guéron [27], for the experimental conditions encountered in the present context, the theory can conveniently be expressed in terms of a complex function $\theta(E)$ and a real function $\phi(E)$.

The retarded and advanced Green's functions are expressed geometrically by two matrices,

$$\hat{G}^R = \begin{pmatrix} \cos \theta & e^{-i\phi} \sin \theta \\ e^{i\phi} \sin \theta & -\cos \theta \end{pmatrix}$$

and

$$\hat{G}^A = \begin{pmatrix} -\cos \bar{\theta} & e^{-i\phi} \sin \bar{\theta} \\ e^{i\phi} \sin \bar{\theta} & \cos \bar{\theta} \end{pmatrix},$$

where $\theta = \theta(r, E)$ is a complex angle which is a measure of the pairing, called the pairing angle for short, and $\phi = \phi(r, E)$ is the superconducting phase, a real quantity. With these variables, one can express quantities familiar from the Ginzburg-Landau theory such as the supercurrent J_s and the density of superconducting electrons $|\Psi|^2$ in terms of microscopic variables. For the supercurrent, we have

$$j_s = \frac{\sigma_N}{e} \int_{-\infty}^{+\infty} dE \tanh \left(\frac{E}{2k_B T} \right) \text{Im} \sin^2 \theta \left(\nabla \phi - \frac{2e\vec{A}}{\hbar} \right), \quad (2)$$

and for the density of superconducting electrons, we have

$$|\Psi|^2 = \frac{m}{e^2 \hbar} \sigma_N \int_0^{+\infty} dE \tanh \left(\frac{E}{2k_B T} \right) \text{Im} \sin^2 \theta. \quad (3)$$

Here, $\sigma_N = e^2 N_0 D$ is the normal-state conductivity, where N_0 is the density of states in the normal state, including spin, and D is the diffusion coefficient; m is the electron mass. The second quantity makes it clear that the density of superconducting electrons is determined by $\text{Im}[\sin^2 \theta]$, which is equivalent to an effective energy-dependent density of pairs. The integration over the energies weighted by the Fermi-Dirac distribution determines the averaged quantity $|\Psi|^2$. So, for a proper understanding of the response of the superconductor, one needs to know $\theta(E)$ and $\phi(E)$. The kinetic inductance is determined by the

density of superconducting electrons through

$$L_k = \frac{m}{e} \frac{1}{e\sigma_N |\Psi|^2}, \quad (4)$$

which illustrates that the nonlinear response of the kinetic inductance is due to a change in the density of superconducting electrons, which in turn is determined by the energy-dependent pairing angle θ . The single-particle density of states, which is the quantity which is measured with a tunnel junction, is given by

$$N(r, E) = N_0 \text{Re} \cos \theta(r, E). \quad (5)$$

A. dc currents and microwave currents

For a stationary current-carrying superconductor, Anthore *et al.* [17] have shown that the quantities θ and ϕ are determined by two basic equations:

$$E + i\Gamma \cos \theta = i\Delta \frac{\cos \theta}{\sin \theta} \quad (6)$$

and

$$\vec{\nabla}(\vec{v}_s \sin^2 \theta) = 0, \quad (7)$$

where $\vec{v}_s = D[\vec{\nabla}\phi - (2e/\hbar)\vec{A}]$ and Γ is given by $(\hbar/2D)v_s^2$. Experimentally, either a magnetic field or a current is imposed, forcing a value for Γ , which then leads to solutions of Eq. (6), i.e., for $\theta(E)$. For later use we rewrite Eq. (6) as

$$iE \sin \theta + \Delta \cos \theta + \alpha_{\text{dc}} \Pi = 0, \quad (8)$$

where α_{dc} is defined as $\Gamma/4$ and $\Pi = 4i \cos \theta \sin \theta = 2i \sin 2\theta$. For $\alpha_{\text{dc}} = 0$, we find the conventional BCS solution. With finite α_{dc} , the BCS density of states is rounded, and a reduced value for the energy gap in the excitation spectrum is obtained. We assume here a uniform current over the cross section of the wire.

The effect of a dc supercurrent and a magnetic field on the superconducting state, i.e., the effect on $\theta(r, E)$, has been measured by Anthore *et al.* [17] by measuring the density of states of a superconductor with a tunnel junction. The results illustrate that for a uniform current density and for a narrow strip in a magnetic field, the response of the superconductor is identical for low current densities. For higher values of α , a difference occurs when the supercurrent reaches the critical pair-breaking current, at which point stable solutions cease to exist. For the magnetic field, solutions continue to exist, decreasing smoothly until a gapless state is reached. The change in $\theta(r, E)$ also enters the kinetic inductance, through Eqs. (3) and (4), leading to an increase in the kinetic inductance due to a reduction in the density of superconducting electrons, which reflects a

reduction in the pairing angle $\theta(r, E)$. At small currents, i.e., $I/I_* \ll 1$, this increase in the kinetic inductance with the current is given by Eq. (1) with $I_* \simeq 2.69I_c$, where the depairing critical current $I_c \simeq 0.75\Delta_u/eR_\xi$ [17], R_ξ is the normal resistance per coherence length $\xi = \sqrt{\hbar D/\Delta_u}$, with Δ_u being the unperturbed value of the energy gap. The zero-current kinetic inductance, in the limit $\Delta_u \gg k_B T$, is given by $L_k(0) = \hbar R_N/\pi \Delta_u$, with R_N being the normal resistance.

An electromagnetic field, defined by the vector potential A , represents the microwave field $A = A_0 \cos(\omega_0 t)$ of frequency ω_0 , which leads to an ac supercurrent. In using the Usadel equations, we assume a dirty superconductor in which the momentum of the electrons is randomized by impurity scattering faster than the relevant processes. We restrict the analysis to small intensities of the rf drive and frequencies less than the unperturbed energy gap Δ_u , i.e.,

$$\alpha \ll \hbar\omega_0 \ll \Delta_u, \quad (9)$$

where the parameter α is the normalized intensity of the rf drive [28], defined by $\alpha = e^2 D A_0^2 / 4\hbar$. The inequalities in Eq. (9) impose the same restriction on α , ω_0 , and Δ_u as used previously by Semenov *et al.* [13], which means that the conditions for the ‘‘quantum mode of depairing’’ are fulfilled [29]. We assume that the temperature is low, $k_B T \ll \Delta_u$, and hence the number of thermal quasiparticles at energies of the order of Δ_u is negligible. When evaluating the tunnel-relaxation model, we also assume that $\alpha \ll \Gamma_{\text{inel}}$, which is a technical assumption required to apply a linear expansion of the Green’s functions in α , and does not affect any of our results qualitatively.

The response to an ac current of frequency ω_0 in the microwave range has been presented by Semenov *et al.* [13], and, rewritten in the variables θ and ϕ , it leads again to Eq. (8) with $\alpha_{\text{dc}} \rightarrow \alpha$ and the function Π replaced by

$$\Pi = i \sin \theta (\cos \theta_+ + \cos \theta_-) + i \cos \theta (\sin \theta_+ + \sin \theta_-), \quad (10)$$

where the subscripts represent the argument being $E + \hbar\omega_0$ or $E - \hbar\omega_0$. This represents the moving superconducting condensate due to the oscillating microwave currents.

To facilitate a comparison with experimentally more accessible values, we express α/Δ_u in terms of the induced rf supercurrent I_{rf} . We can relate the amplitude of the induced current I_0 and the field by $L_{k,u} I_0 = A_0$, where $L_{k,u}$ is defined per unit length along the wire. This is just Eq. (2) in the limit of a small current density, without the phase gradient. We arrive at

$$\frac{\alpha}{\Delta_u} = \frac{1}{2\pi^2} \frac{\langle I_{\text{rf}}^2 \rangle}{(\Delta_u/eR_\xi)^2} \simeq 0.028 \frac{\langle I_{\text{rf}}^2 \rangle}{I_c^2}, \quad (11)$$

by expressing α through I_{rf} as $\alpha = e^2 D (L_{k,u} I_0)^2 / 4\hbar = e^2 D (L_{k,u})^2 \langle I_{\text{rf}}^2 \rangle / 2\hbar$, with $\langle I_{\text{rf}}^2 \rangle = I_0^2 / 2$ being the mean square of the induced rf current.

B. Inelastic scattering

At any finite temperature, the presence of microwaves results in an absorption of microwave energy by electrons, which needs to be balanced by an inelastic scattering process. Hence, in the kinetic equation we take inelastic scattering into account, which, for consistency, should also be studied for the spectral properties. In Ref. [13], this was not done explicitly, with the assumption that the presence of quasiparticle relaxation was used implicitly. Without a strong enough relaxation, the distribution function cannot have the equilibrium form assumed in previous work. Inelastic scattering is introduced by assuming a relaxation-time approximation, which is equivalent to taking the self-energy to be of the form [30,31]

$$\check{\Sigma}_{\text{inel}} = -i\Gamma_{\text{inel}}\check{G}_{\text{res}}, \quad (12)$$

where Γ_{inel} is the tunneling rate and \check{G}_{res} is the Green's function of an equilibrium "reservoir" to which the "hot electrons" tunnel. Formally, this model corresponds to the relaxation-time approximation. In principle, it can be compared to a thin-film superconductor coupled to a large normal reservoir via a tunnel barrier with transparency, equivalent to a tunneling rate equal to Γ_{inel} . While, under realistic conditions, tunnel coupling to a reservoir is not the mechanism of energy relaxation, it is a very useful and tractable model, which captures the essential physics. Its predictions about the effect of the microwave drive on the spectral functions remain qualitatively correct for the case of electron-electron or electron-phonon interaction inside the superconductor. Moreover, as we will discuss below, the effect of the ac drive on quantities such as the order parameter and the kinetic inductance are insensitive to the details of the superconductor's spectral properties introduced by the inelastic processes. Hence, the corresponding results derived with the chosen model are correct quantitatively.

In terms of the pairing angle θ , one obtains

$$(iE - \Gamma_{\text{inel}}) \sin \theta + \Delta \cos \theta + \alpha \Pi = 0. \quad (13)$$

This expression provides solutions for $\theta(E)$ for a given value of α and a material-dependent inelastic scattering rate Γ_{inel} . A typical result for the density of states, Eq. (5), is shown in Fig. 1 using results to be presented in the next section.

C. Analytical results

Employing the self-energy in Eq. (12), one arrives at the kinetic equation for the stationary longitudinal components

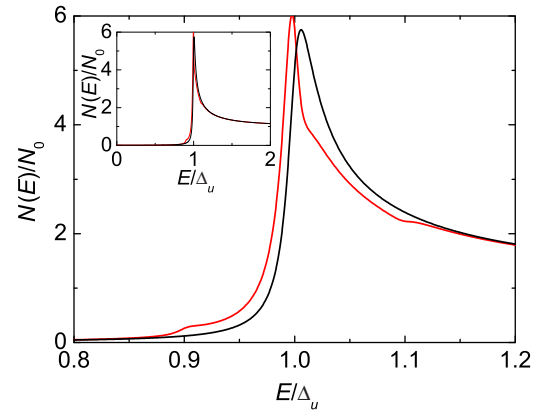


FIG. 1. Normalized DOS of a superconductor $N(E)/N_0 = \text{Re}[\cos \theta(E)]$ with $\alpha/\Delta_u = 10^{-3}$ and $\hbar\omega_0/\Delta_u = 0.1$ on an expanded energy scale. The red curve is for the case with radiation and the black curve for the case without. A total inelastic parameter $\Gamma_{\text{inel}}/\Delta_u = 0.01$ is assumed. The inset shows the full density of states, making it clear that the deviations are small, but observable enough to allow one to evaluate the conceptual framework.

[21–23] of the quasiparticle distribution function f_L :

$$I_{\text{phot}}[f_L] + I_{\text{inel}}[f_L] = 0. \quad (14)$$

Here, the electron-photon collision term I_{phot} describes the creation of quasiparticles and the absorption of energy, and the inelastic scattering term I_{inel} provides quasiparticle and energy relaxation. The integral of the electron-photon collisions is given by

$$I_{\text{phot}} = \alpha [R_+ (f_L - f_{L+}) + R_- (f_L - f_{L-})], \quad (15)$$

where $R_{\pm} = \text{Re}[\cos \theta_{\pm}] + \text{Im}[\sin \theta] \text{Im}[\sin \theta_{\pm}] / \text{Re}[\cos \theta]$ (more details of the derivation of this electron-photon collision integral can be found in Ref. [32]).

The integral of the inelastic collisions in the relaxation-time approximation is

$$I_{\text{inel}} = \Gamma_{\text{inel}} (f_L - f_{L,\text{res}}) = \Gamma_{\text{inel}} \delta f_L, \quad (16)$$

in which $f_{L,\text{res}}$ is the distribution function of the quasiparticles in the "reservoir," which is assumed to be in equilibrium at a base temperature T . The subscript L is a reminder that only a longitudinal type of nonequilibrium, symmetric around E_F , is relevant [10].

The set of equations (13) and (14) is closed by the self-consistency equation, which has the usual form,

$$\Delta = \lambda \int_0^{\hbar\omega_D} d\varepsilon f_L \text{Im} \sin \theta, \quad (17)$$

where ω_D is the Debye frequency and λ is the electron-phonon coupling constant.

The linearization of Eq. (13) gives

$$(E + i\Gamma_{\text{inel}})\delta \sin \theta - i\Delta_u \delta \cos \theta - i \cos \theta_u \delta \Delta + \alpha \Pi_u = 0, \quad (18)$$

where $\delta \sin \theta \equiv \sin \theta - \sin \theta_u$ and $\delta \cos \theta \equiv \cos \theta - \cos \theta_u$. Here, θ_u denotes the unperturbed solution without an rf drive, for $\alpha = 0$, and is given by

$$\cos \theta_u = \frac{(E + i\Gamma_{\text{inel}})}{\{(E + i\Gamma_{\text{inel}})^2 - \Delta_u^2\}^{1/2}} \equiv \frac{(E + i\Gamma_{\text{inel}})}{\Xi}, \quad (19)$$

$$i \sin \theta_u = \frac{-\Delta_u}{\{(E + i\Gamma_{\text{inel}})^2 - \Delta_u^2\}^{1/2}} \equiv -\frac{\Delta_u}{\Xi}, \quad (20)$$

where Δ_u is the value of the order parameter for no rf drive, and $\Xi \equiv \{(E + i\Gamma_{\text{inel}})^2 - \Delta_u^2\}^{1/2}$. In the limit of $\Gamma_{\text{inel}} \rightarrow 0$, the unperturbed functions in Eqs. (19) and (20) reduce to the standard BCS solution [21–23]. The finite Γ_{inel} describes the broadening of the spectral functions of the superconductor due to the inelastic processes [33].

The solution of the linearized Eq. (18) has the form

$$i\delta \sin \theta = i \frac{\partial \sin \theta}{\partial \Delta} \Big|_{\alpha=0} \delta \Delta + i \frac{\partial \sin \theta}{\partial \alpha} \Big|_{\Delta=\Delta_u} \alpha, \quad (21)$$

$$\delta \cos \theta = \tan \theta_u \delta \sin \theta = \frac{\Delta_u}{E + i\Gamma_{\text{inel}}} i\delta \sin \theta. \quad (22)$$

The partial derivatives are given by

$$\begin{aligned} i \frac{\partial \sin \theta}{\partial \alpha} \Big|_{\Delta=\Delta_u} &= \frac{i\Delta_u \{(E_+ + i\Gamma_{\text{inel}}) + (E + i\Gamma_{\text{inel}})\} (E + i\Gamma_{\text{inel}})}{\Xi_+ \Xi^3} \\ &+ \{E_+ \rightarrow E_-\} \end{aligned} \quad (23)$$

and

$$i \frac{\partial \sin \theta}{\partial \Delta} \Big|_{\alpha=0} = \frac{-(E + i\Gamma_{\text{inel}})^2}{\Xi^3}. \quad (24)$$

Equation (21) expresses the linear change in the Green's function $\delta \sin \theta$ under the influence of the rf drive as a sum of two terms: one proportional to the normalized rf drive intensity α , and another proportional to the variation of the order parameter $\delta \Delta$.

Since the change in the order parameter is determined in part by the nonequilibrium distribution function of the quasiparticles, we first determine this quantity from the kinetic equation. Just for simplicity, we restrict our derivations here to the limit $k_B T \ll \hbar\omega_0$ (later, we remove this restriction). Then the differences $f_{L,u} - f_{L\pm,u}$ are different from zero only in the small energy interval $-\hbar\omega_0 <$

$E < \hbar\omega_0$, where $\text{Re} \cos \theta_u \cong \text{Re} \cos \theta_{\pm,0} \cong \Gamma_{\text{inel}}/\Delta_u$ and $\text{Re} \sin \theta_u \cong (\Gamma_{\text{inel}}/\Delta_u) (E/\Delta_u) \ll \text{Re} \cos \theta_u$. Hence, the electron-photon collision integral (15) can be simplified to $I_{\text{phot},u} = \alpha (\Gamma_{\text{inel}}/\Delta_u) \{(f_{L,u} - f_{L+,u}) + (f_{L,u} - f_{L-,u})\}$. Then the solution of the kinetic equation (14) has the following form:

$$\delta f_L = \frac{\partial f_L}{\partial \alpha} \Big|_{\Delta=\Delta_u} \alpha, \quad (25)$$

where

$$\frac{\partial f_L}{\partial \alpha} \Big|_{\Delta=\Delta_u} = \begin{cases} -2/\Delta_u, & E \in (0, \hbar\omega_0) \\ 2/\Delta_u, & E \in (-\hbar\omega_0, 0) \\ 0, & E \notin (-\hbar\omega_0, \hbar\omega_0) \end{cases}. \quad (26)$$

Note that, with the chosen model of relaxation [Eq. (12)], the quantity which characterizes the strength of the inelastic interaction, Γ_{inel} , drops out of the answer. The reason is that both collision integrals in the kinetic equation (14) are proportional to Γ_{inel} .

The linearization of the self-consistency equation (17) leads to the following relation for the small correction to the order parameter $\delta \Delta$:

$$\delta \Delta = \delta_\theta \Delta + \delta_{f_L} \Delta, \quad (27)$$

where

$$\delta_\theta \Delta = \alpha \int_0^\infty dE \frac{\partial \text{Im}[\sin \theta]}{\partial \alpha} \Big|_{\Delta=\Delta_u} f_{L,u} \quad (28)$$

and

$$\delta_{f_L} \Delta = \alpha \int_0^\infty dE \text{Im}[\sin \theta_u] \frac{\partial f_L}{\partial \alpha} \Big|_{\Delta=\Delta_u}. \quad (29)$$

Here, Eq. (28) describes the change in the order parameter Δ due to the change in the anomalous Green's function $\sin \theta$, and Eq. (29) describes the change due to the change in the distribution function f_L .

Substituting into Eqs. (28) and (29) the formulas for $\partial_\alpha \sin \theta|_{\Delta=\Delta_u}$ [Eq. (23)] and $\partial_\alpha f_L|_{\Delta=\Delta_u}$ [Eq. (26)] makes it possible to calculate these corrections analytically. Taking into account the fact that the integrand in Eq. (29) is analytic in the upper half of the complex plane and decays faster than $1/E$ at infinity, we replace the integration over the real semiaxis $E \in (0, +\infty)$ with an integration over the imaginary semiaxis $iE \in (0, +i\infty)$ and obtain, after

dropping terms of nonzero order in $\Gamma_{\text{inel}}/\Delta_u$ and $\hbar\omega_0/\Delta_u$,

$$\frac{\delta_\theta \Delta}{\alpha} \cong \int_0^\infty dy \frac{4y^2}{\{y^2 + 1\}^2} = -\pi. \quad (30)$$

The correction to Δ due to the change in f_L turns out to be small,

$$\frac{\delta_{f_L} \Delta}{\alpha} \cong -\frac{\Gamma_{\text{inel}}}{\Delta_u} \int_0^{\hbar\omega_0/\Delta_u} x dx \simeq -\left(\frac{\hbar\omega_0}{\Delta_u}\right)^2 \frac{\Gamma_{\text{inel}}}{\Delta_u}, \quad (31)$$

and can be neglected compared with $\delta_\theta \Delta$. Finally, we obtain

$$\frac{\delta \Delta}{\Delta_u} \cong -\pi \frac{\alpha}{\Delta_u}. \quad (32)$$

The change in the distribution function δf_L , given by Eqs. (25) and (26) has a minor effect on $\delta \Delta$ because δf_L is nonzero only in the small energy interval $E \in (-\hbar\omega_0, \hbar\omega_0)$, where $\text{Im} \sin \theta_u$ is small. It is obvious that the same holds if the temperature is not small compared with $\hbar\omega_0$ (but still small compared with Δ_u). In the case $\hbar\omega_0 \ll k_B T \ll \Delta_u$, δf_L is nonzero at roughly $E \in (-k_B T, k_B T)$. Hence, in the formula for $\delta_{f_L} \Delta$ one has to replace $(\hbar\omega_0/\Delta_u)^2$ by approximately $(k_B T/\Delta_u)^2$, which is also a small factor.

The main results we obtain with this simplest possible model of inelastic processes are (i) the formulas for the rf-drive-induced corrections to spectral functions and to the order parameter in Eqs. (21) and (32), and (ii) a statement about the smallness of the effect of the rf-drive-induced nonequilibrium in the quasiparticle subsystem on the spectral functions.

III. SUPERCONDUCTING DENSITY OF STATES AND MICROWAVES

The solution of Eqs. (13) and (17) provides the superconducting properties expressed in $\theta(E)$, which is dependent on the microwave frequency ω_0 and intensity α . The most direct manifestation of this change due to the embedded microwave field is a change in the DOS, as defined in Eq. (5). Previously, we have presented [13] results for the modified DOS for the case without inelastic processes, which physically corresponds to $\Gamma_{\text{inel}} \ll \alpha$. Here, we expand on those results by also calculating the change in the DOS for the opposite case, $\Gamma_{\text{inel}} > \alpha$.

The change in the density of states is given by $\delta N = N_0 \text{Re}[\delta \cos \theta]$, with $\delta \cos \theta$ given by Eq. (22). It consists of two terms, both proportional to the normalized field

intensity:

$$\delta N = \frac{\partial N}{\partial \alpha} \alpha - \frac{\partial N}{\partial \Delta} \frac{\pi}{\Delta_u} \alpha. \quad (33)$$

The terms have different physical meanings. The first term is the one of main interest, because it describes a qualitative modification of the DOS due to the embedded microwave field. Its magnitude is given by

$$\frac{\partial N}{\partial \alpha} = N_0 \text{Re} \left[\frac{i\Delta_u^2 \{(E_+ + i\Gamma_{\text{inel}}) + (E + i\Gamma_{\text{inel}})\}}{\Xi_+ \Xi^3} \right] + \{E_+ \rightarrow E_-\}. \quad (34)$$

Because of the factors $\Xi_\pm = \left\{ (E \pm \hbar\omega_0 + i\Gamma_{\text{inel}})^2 - \Delta_u^2 \right\}^{1/2}$ in the denominator, it has features near the ‘‘photon point’’ energies $\Delta_u \mp \hbar\omega_0$. Near these energies, Eq. (34) can be approximated as

$$\frac{\partial N}{\partial \alpha} = N_0 \frac{\Delta_u^2 \left[(E_\pm - \Delta_u) + \left\{ (E_\pm - \Delta_u)^2 + \Gamma_{\text{inel}}^2 \right\}^{1/2} \right]^{1/2}}{(2\hbar\omega_0)^{3/2} \left\{ (E_\pm - \Delta_u)^2 + \Gamma_{\text{inel}}^2 \right\}^{1/2}}. \quad (35)$$

Its maximum scales as $2^{-3/2} (\Gamma_{\text{inel}}/\Delta_u)^{-1/2} (\hbar\omega_0/\Delta_u)^{-3/2}$, and the width of the maximum is given by Γ_{inel} .

The second term of Eq. (33),

$$\frac{\partial N}{\partial \Delta} = -N_0 \frac{\Delta_u (E + i\Gamma_{\text{inel}})}{\Xi^3}, \quad (36)$$

describes the shift of the DOS due to the suppression of the order parameter Δ under the influence of the microwave field. It does not contain the photon energy $\hbar\omega_0$.

The total change in the DOS [Eq. (33)] is presented in Fig. 2, for a fixed frequency $\hbar\omega_0 = 0.1\Delta_u$ and a fixed $\alpha = 10^{-3}\Delta_u$. The change is normalized to the normal-state DOS. The inelastic collision strength $\Gamma_{\text{inel}}/\Delta_u$ is varied from 0.003 (red) and 0.01 (green) to 0.03 (blue). The curve for the smallest value of this quantity almost coincides with the unperturbed curve (black), calculated within the approach published previously [13]. This indicates that the violation of the condition $\alpha \ll \Gamma_{\text{inel}}$, which was needed to apply the linear expansion in α near the peaks at Δ_u and $\Delta_u \pm \hbar\omega_0$, does not affect significantly the results for the spectral functions, confirming that this condition is in practice not important. It is clear that the inelastic processes reduce the visibility of the photon structures in the density of states. However, a quantitative analysis of the behavior of Eq. (33) shows that the extrema in $\text{Re} \delta \cos \theta(E)$ near $\Delta_u \pm \hbar\omega_0$ exist up to $\Gamma_{\text{inel}}/\hbar\omega_0 \approx 0.15$ (for $\hbar\omega_0 \ll \Delta_u$). Hence, in principle, the photon steps should be clearly discernible, provided a high enough accuracy can be obtained

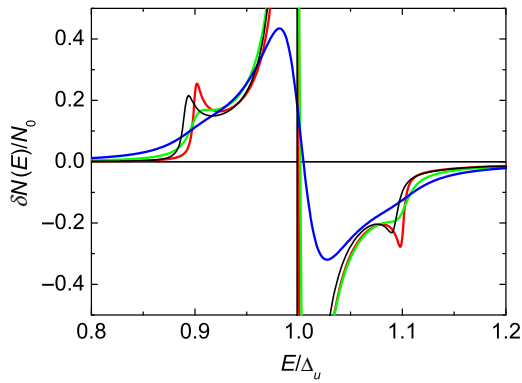


FIG. 2. Change in normalized DOS of a superconductor, $\delta N(E)/N_0 = \text{Re}[\delta \cos \theta(E)]$, under the influence of an rf drive with $\alpha/\Delta_u = 10^{-3}$. The black curve corresponds to the absence of relaxation, the red curve corresponds to a value of the relaxation rate $\Gamma_{\text{inel}}/\Delta_u = 0.003$, the green curve corresponds to $\Gamma_{\text{inel}}/\Delta_u = 0.01$, and the blue curve corresponds to $\Gamma_{\text{inel}}/\Delta_u = 0.03$.

in an experiment and sufficiently low temperatures are used.

The most important quantity for kinetic induction detection and parametric amplification is the nonlinear kinetic inductance, as expressed below in Eq. (46). It is a clear experimental signature of how the microwave intensity becomes embedded in the Cooper-pair condensate. From a practical point of view, that particular result is directly usable in a model. Unfortunately, it is not very informative about the influence of the microwave field on the microscopic properties of the superconductor and the dependence on the material properties. A much more critical test would be a direct measurement of the density of states in the presence of microwaves.

Here, we propose an experiment in which the rf-driven superconducting properties are measured with a tunnel junction. It is well known that tunnel junctions are very suitable for determining the density of states, as well as the Fermi distribution function, of a superconductor. However, the challenge is to design an experiment in which only one of the electrodes is driven by the microwave field, and not the other electrode. In addition, one wants to avoid the possibility that during the measurement by use of the tunneling current the tunneling process is modified by photon-assisted tunneling (PAT) [34]. This problem plagued early experiments by Kommers and Clarke [35] and led to some early solutions by Horstman and Wolter [36,37]. The experimental challenge is to avoid or minimize any rf field across the tunnel barrier, using present-day fabrication technology and design tools. Figure 3 shows our proposed experiment, which takes these considerations into account.

Our proposed circuit can be divided into two parts, which are shown in black and gray in Fig. 3. The black layer is a superconductor, for instance aluminum, patterned

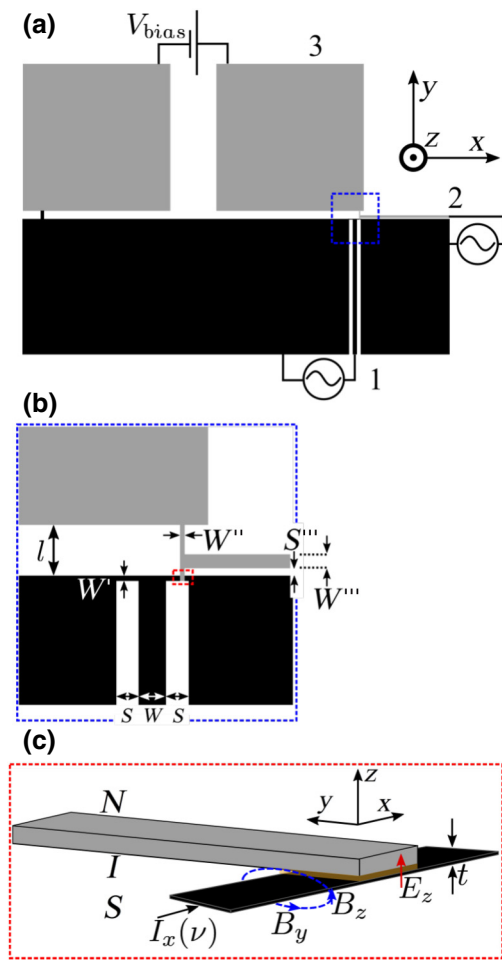


FIG. 3. (a) Proposed device to test the theoretical model. The black layers are patterned in a superconductor, whereas the gray layers are patterned in a normal metal. The circuit lies in the x - y plane of the coordinate system indicated. (b) Enlargement of the region around the normal-metal–insulator–superconductor tunnel junction. (c) Side view of the tunnel junction (dark red), specifying the electric and magnetic fields created by the rf current $I_x(\nu)$ at the driving frequency $\nu = \omega_0/2\pi$. The tunnel junction is used to probe the coherent excitation of the (black) superconducting wire beneath the tunnel junction by means of a density-of-states measurement of the wire. The circuit sketch in (a),(b) is drawn to scale.

as indicated in the figure. The gray layer is made of a normal-conducting metal, for instance copper. The dashed blue box in Fig. 3(a) indicates the region where a normal-metal–insulator–superconductor (N - I - S) tunnel junction is formed between the black and gray metals. This region is shown in more detail in Fig. 3(b). The N - I - S tunnel junction is formed at the overlap of the black superconducting wire, with a width $W' = 1 \mu\text{m}$ and thickness $t = 20 \text{ nm}$, and the gray wire, with a width $W'' = 1 \mu\text{m}$. The latter normal-metal wire has a total length of $l = 21 \mu\text{m}$ and acts as an inductance, just large enough, $L \approx 15 \text{ pH}$, to block the rf currents $I_x(\nu)$ to the N - I - S junction. Through this,

we prevent the rf currents propagating into the junction and coupling into the measurement circuitry attached to it. This signal blockage works well in combination with an effectively shorted wire (black layer) on which the junction is patterned, as explained in more detail in the following paragraph. At the same time, the length of normal-metal wire that is connected to the N - I - S junction is short enough to avoid a relevant series resistance, which is added to the overall tunnel resistance of the junction. For a copper wire of the chosen dimensions with a common thin-film resistivity of $\rho_0 = 0.4 \mu\Omega \text{ cm}$ [38], one expects about 0.02Ω of series resistance. The tunnel resistance of the N - I - S junction should therefore have a value much larger than this series resistance, which is compatible with the use of an opaque tunnel barrier to probe the superconducting properties. The N - I - S tunnel junction is connected to three measurement terminals, labeled 1–3 in the figure. These make it possible to probe the dc tunneling curve of the N - I - S junction, while the states in the superconducting wire of width W' underneath the tunnel junction can be probed. Although in our device proposal the N - I - S tunnel junction has an area of $1 \mu\text{m}^2$, a smaller tunnel junction would equally well suffice to perform the experiment and would only insignificantly modify the circuit functionality. Therefore, our design is compatible with the established trilayer and angle-evaporation junction fabrication techniques, which can realize junctions of different sizes.

Terminal 1 is connected to an rf generator and is used to excite a transverse electromagnetic (TEM) wave on a coplanar-waveguide (CPW) transmission line at frequencies of up to 60 GHz. The CPW is designed to have a characteristic impedance of $Z_c = 50 \Omega$, which we achieve by choosing the CPW dimensions to be $S = 8 \mu\text{m}$ and $W = 11 \mu\text{m}$, on top of a $275 \mu\text{m}$ thick silicon wafer, ignoring the natural oxide layer on the silicon about 1 nm thick. The CPW is terminated in a short circuit by a superconducting wire of width W' at the position of the N - I - S junction. The short circuit results in a maximum rf current $I_x(\omega_0)$, which is homogeneous, in the wire and drives the superconducting ground state in the wire at a particular frequency, ω_0 , and with a certain magnitude of the rf current which can be adjusted by the rf generator. We find by modeling our circuit in CST [39] that at the tunnel-junction barrier a magnetic and an electric field are established due to the rf driving, as sketched schematically in Fig. 3(c). We design the circuit in such a way as to minimize primarily the electric field component E_z established across the junction, which would lead to unwanted PAT currents. If they were too large in magnitude, the PAT currents would overwhelm the features due to the coherently excited density of states, created on purpose by the rf drive from terminal 1. For an rf-drive power of -20 dBm at terminal 1, we find that the rf current which passes through the superconducting wire at the position of the tunnel junction will create a

magnetic field of $B_y, B_z < 1 \text{ G}$ at the tunnel barrier. Hence, it will only slightly disturb the superconducting ground state that we want to study. For the same drive power, we expect additionally a buildup of an electric (stray) field E_z across the junction which on average will amount to 4.5 V/m , leading to a parasitic voltage drop of only 4.5 nV across the junction for a tunnel barrier of thickness 1 nm . Depending on the differential resistance of the N - I - S junction under the rf drive, of the order of several 100Ω , this will cause only a negligible parasitic tunnel current. The values of the magnetic and electric fields are determined for an excitation frequency of $\omega_0/2\pi = 15 \text{ GHz}$, but will change only slightly for other frequencies. Although it is not specified in the figure, we envision that the rf generator will be connected through a circulator or a directional coupler to terminal 1. This way, we prevent the buildup of a standing wave due to reflection of the TEM wave at the wire terminating the CPW.

A second rf generator can be connected to terminal 2 and can be employed to excite a quasi-TEM wave on a coplanar-strip (CPS) transmission line which is connected to the N - I - S junction from the right side. One part of the CPS transmission line connects to the S part and the other part connects to the N part of the N - I - S junction; hence, an rf current is driven on purpose through the junction, leading to a controlled PAT current. This allows one to disentangle possible PAT features which might be introduced by exciting the circuit from terminal 1 and which might disturb the density-of-states and distribution-function measurements. The CPS transmission line has a characteristic impedance equal to $Z_c = 50 \Omega$, which we achieve by choosing the dimensions $S''' = 3 \mu\text{m}$ and $W''' = 7 \mu\text{m}$. We suggest using a normal metal for the part of the CPS which connects to the N part of the N - I - S junction in order to prevent the proximity effect modifying the density of states in the N - I - S junction. Similarly to the rf excitation from terminal 1, we also suggest that the rf generator at terminal 2 should be connected through a circulator or a directional coupler.

Finally, terminal 3 realizes the dc-bias or low-frequency part of the circuit, which can be used to voltage bias the N - I - S junction or to apply a low-frequency bias modulation for lock-in measurements of the differential resistance. The latter measurement yields a convolution of the density of states with the distribution function of the two N - I - S junction electrodes, which are both unknown, but could be disentangled by a proper analysis of the measurements obtained for different drive powers. For the same reason, we propose to use an asymmetric N - I - S junction for the deconvolution procedure. Also, because of the voltage applied to the N - I - S junction, we suggest using dc blocks at terminals 1 and 2 to protect the rf generators.

To fully characterize our device proposal, we need to quantify also the isolation of the three terminals from each other when an rf excitation is applied to them. In our

circuit simulation, we find reasonable isolation values of less than -20 dB for S_{21} , S_{31} , S_{12} , and S_{32} for an operation frequency band of 2–60 GHz. Therefore we believe that, using currently available technology, an evaluation of the microscopic properties of a superconductor in the presence of microwaves is feasible.

IV. NONLINEAR SUPERCONDUCTING KINETIC INDUCTANCE

Another quantity which is important for microwave kinetic inductance detectors and parametric amplifiers, and which is determined by the change in spectral properties and/or the distribution function, is the complex conductivity σ at a frequency ω . It is given by

$$\begin{aligned} \sigma(\omega) = & \frac{\sigma_N}{4\hbar\omega} \int dE ((\cos\theta_- \operatorname{Re} \cos\theta \\ & + i \sin\theta_- \operatorname{Re} [i \sin\theta]) f_L - \{(\cos\theta)^* \operatorname{Re} \cos\theta_- \\ & + (i \sin\theta)^* \operatorname{Re} [i \sin\theta_-]\} f_{L-}). \end{aligned} \quad (37)$$

The imaginary part of the conductivity, measurable through the kinetic inductance L_k , is given by the relationship $L_k = 1/\omega \operatorname{Im} \sigma$. Equation (37) is a generalization of the Mattis-Bardeen relation [40] for the case of not only nonequilibrium distribution functions, as was done by Catelani *et al.* [41], but also for changed spectral functions. For low frequencies $\hbar\omega \ll \Delta_u$, the equation for the imaginary part of the conductivity (37) reduces to

$$\operatorname{Im}[\sigma(\omega \ll \Delta/\hbar)] = \operatorname{Im} \sigma_0 = -\frac{\sigma_N}{\hbar\omega} \int dE \operatorname{Im} [\sin^2 \theta] f_L. \quad (38)$$

The unperturbed value of $\operatorname{Im} \sigma(\omega \ll \Delta/\hbar)$ is given by

$$\operatorname{Im} \sigma_{0,u} = \sigma_N \frac{\Delta_u}{\hbar\omega} \pi, \quad (39)$$

which is a form of the above-mentioned well-known relation between the kinetic inductance and normal resistance [4,10].

The small correction to the kinetic inductance at low frequencies ($\hbar\omega \ll \Delta_u$), i.e., the case of microwave radiation with commonly used superconductors, is the sum of two terms:

$$\frac{\delta L_k}{L_{k,u}} = \frac{\delta_\alpha L_k}{L_{k,u}} + \frac{\delta_\Delta L_k}{L_{k,u}}. \quad (40)$$

The first term describes the change in the kinetic inductance due to the change in the spectral and distribution

functions under the influence of the rf drive,

$$\frac{\delta_\alpha L_k}{L_{k,u}} = -\frac{1}{\operatorname{Im} \sigma_{0,u}} \frac{\partial \operatorname{Im} \sigma_0}{\partial \alpha} \Big|_{\Delta=\Delta_u} \alpha, \quad (41)$$

whereas the second term describes the change in the kinetic inductance due to the change in the order parameter Δ ,

$$\frac{\delta_\Delta L_k}{L_{k,u}} = -\frac{1}{\operatorname{Im} \sigma_{0,u}} \frac{\partial \operatorname{Im} \sigma_0}{\partial \Delta} \Big|_{\alpha=0} \delta\Delta. \quad (42)$$

Because of Eq. (39), the second term, Eq. (42), is equal to $\delta_\Delta L_k/L_{k,u} = -\delta\Delta/\Delta_u$ and is given by Eq. (32). The first term, Eq. (41), is evaluated using Eq. (38) for the imaginary part of the conductivity:

$$\begin{aligned} \frac{\delta_\alpha L_k}{L_{k,u}} = & \\ = & \left(\int dE \frac{\partial \operatorname{Im} \sin^2 \theta}{\partial \alpha} f_{L,u} + \int dE \operatorname{Im} [\sin^2 \theta_u] \frac{\partial f_L}{\partial \alpha} \right) \Big|_{\Delta=\Delta_u} \alpha. \end{aligned} \quad (43)$$

The second integral in this equation, which describes the contribution due to the change in the distribution function, is negligible for the same reason as for the analogous contribution to $\delta\Delta$ in Eq. (27). The first integral in Eq. (43) can be evaluated analytically in a way analogous to that used for Eq. (28), by taking into account Eqs. (20) and (23) and replacing E by iE :

$$\begin{aligned} & \left(\int_0^\infty dE \frac{\partial \operatorname{Im} \sin^2 \theta}{\partial \alpha} f_{L,u} \right) \Big|_{\Delta=\Delta_u} \\ & \cong - \int_0^\infty dy \frac{8y^2}{\{y^2 + 1\}^{5/2}} = -\frac{8}{3}. \end{aligned} \quad (44)$$

Substituting this into the first term of Eq. (43), we obtain

$$\frac{\delta_\alpha L_k}{L_{k,u}} = \frac{16}{3\pi} \frac{\alpha}{\Delta_u}, \quad (45)$$

and, finally,

$$\frac{\delta L_k}{L_{k,u}} = \left(\frac{16}{3\pi} + \pi \right) \frac{\alpha}{\Delta_u} \simeq 4.84 \frac{\alpha}{\Delta_u}. \quad (46)$$

To facilitate comparison with Eq. (1), we rewrite Eq. (46) in terms of $\langle I_{\text{rf}}^2 \rangle / I_*^2$, using Eq. (11):

$$L_k \langle I_{\text{rf}}^2 \rangle \approx L_k(0) [1 + \langle I_{\text{rf}}^2 \rangle / I_*^2], \quad (47)$$

where $I_* = \sqrt{2}(16/3\pi + \pi)^{-1/2} \pi \Delta_u / eR_\xi \simeq 2.02 \Delta_u / eR_\xi \simeq 2.69 I_c$, exactly as in the dc case.

The correction to the kinetic inductance in Eq. (46), as well as the correction to the order parameter $\delta\Delta/\Delta_u$ in Eq. (32), agrees with the values found in previous numerical calculations [13], despite the qualitative difference between the unperturbed Green's functions, as well as between the corrections to them in the presence of the rf drive $\delta\sin\theta$ and $\delta\cos\theta$. In our view, this agreement has the following reason. The corrections to Δ and L_k , as well as to other quantities which are calculated as integrals of some spectral functions in infinite or semi-infinite limits (and hence are not sensitive to the value of Γ_{inel}), are expected to be the same when calculated in both models. This is despite the fact that the linearization procedure presented in this paper requires $\alpha \ll \Gamma_{\text{inel}}$, whereas the derivations in Ref. [13] correspond to the opposite limit, $\Gamma_{\text{inel}} \ll \alpha$. This indicates that introduction of Γ_{inel} in Eq. (13) can be considered, formally, as a trick which allows linearization with respect to the ratio α/Δ_u . It shifts the poles of the Green's functions away from the real axis and removes singularities, which would render the linearization unfeasible.

There is one more (and deeper) consequence of the above-mentioned independence of this type of integral quantity from the exact position of the poles. In the final formulas, neither Γ_{inel} nor $\hbar\omega_0$ matters, i.e., one can safely replace $E \pm \hbar\omega_0$ by E . Noting that the same replacement (and $\Gamma_{\text{inel}} \rightarrow +0$) in the retarded Usadel equation turns it into the form of the equation for the dc case, with the depairing parameter $\Gamma = 2\alpha$, one sees that the corrections to these integral quantities should be equal in the rf case to those in the dc case. Actually, the results in Eqs. (32) and (46), expressed in terms of the root-mean-square value of the induced rf current ($\delta\Delta/\Delta_u = -0.088 \langle I_{\text{rf}}^2 \rangle / I_c^2$ and $\delta L_k / L_{k,u} = 0.136 \langle I_{\text{rf}}^2 \rangle / I_c^2$), exactly coincide with those for the dc-depairing theory [17], with $\langle I_{\text{rf}}^2 \rangle \rightarrow I_{\text{dc}}^2$. Physically, this means that the time-averaged quantities are sensitive only to the average kinetic energy contained in the supercurrent (the condensate of Cooper pairs), and not to the frequency of its oscillations. We want to stress that this equivalence between the dc and the rf cases does not hold for the integral quantities, which depend not only on spectral functions but also on the distribution functions, such as the real part of the conductivity or the differential conductance of a N - I - S tunnel junction. The inequality $k_B T \ll \hbar\omega_0$ make these latter quantities sensitive to the exact position of the poles at $E \pm \hbar\omega_0$.

We now discuss briefly the applicability of these results to the analysis of kinetic inductance traveling-wave parametric amplifiers [3]. Typically, these devices, exploiting the nonlinearity of the kinetic inductance induced by a strong supercurrent (pump), have to work under the condition $\alpha \ll \hbar\omega_0$. The amplitude of the pump supercurrent I_p does not exceed $I_c/3$, and hence $\langle I_{\text{rf}}^2 \rangle / I_c^2 \simeq 1/20$ and the ratio α/Δ_u is approximately $0.028 \langle I_{\text{rf}}^2 \rangle / I_c^2 \approx 10^{-3}$. For

$\Delta_u/\hbar \simeq 300$ GHz ((Nb,Ti)N or NbN) and $\omega_0/2\pi = 1$ GHz, this yields $\alpha/\hbar\omega_0 \simeq 0.3$, and for $\omega_0/2\pi = 10$ GHz it yields $\alpha/\hbar\omega_0 \simeq 0.03$ (see, for instance Refs. [3], [42], and [43]). At the same time, the simplified model used to describe the operation of these devices assumes that the kinetic inductance is altered as if the current were dc [3], i.e., the model is valid for the opposite case. Hence, the simplified model has to be corrected or confirmed with the use of the theory developed in Ref. [13] and the present theory. To describe the parametric interaction between two weak signals in a transmission line, resonator, or lumped element, the kinetic inductance of which is modulated by a strong pump, one has to know two quantities: the nonlinear correction to the time-averaged admittance or kinetic inductance, which is given by the formula in Eq. (46), and the ‘‘cross-frequency’’ admittance L_{cross} , which is the coefficient relating the current at the frequency ω to the field at the frequency $2\omega_0 - \omega$ (where ω_0 is the frequency of the pump). To find L_{cross} , one needs the components of the spectral functions oscillating at the frequencies $\pm 2\omega_0$. This calculation is beyond the scope of the present paper. Here, we just note that in the case of low frequencies ($\hbar\omega_0 \ll \alpha$), where the dc-case equations are valid, the relationship $L_{\text{cross}} = \delta L_k/2$ holds [3]. For the rf case, which is of interest here, we expect that L_{cross} depends only on α and not on ω_0 , at least as long as $\omega_0 \ll \Delta_u$. Hence, the answer should be $L_{\text{cross}} = \text{const} \times \alpha/\Delta_u = \text{const} \times \delta L_k$, which can differ from the prediction of the theory based on the dc case quantitatively, but not qualitatively.

V. CONCLUSIONS

In summary, we describe theoretically the influence of inelastic processes on coherent excited states of a superconductor [13]. We consider a model in which these processes are represented in the relaxation approximation, which is analogous to exchange of electrons via tunneling to a normal reservoir [30]. We calculate analytically the spectral functions and the nonequilibrium distribution function in the presence of a monochromatic rf drive. We demonstrate that when the conditions for the ‘‘quantum mode of depairing’’ are fulfilled, the change in the kinetic inductance is determined primarily by the change in the spectral functions, and not by the distribution function, which confirms previously published results [13]. We argue that our results have a general meaning, independent of any specific model for the inelastic relaxation. We discuss the implications for kinetic inductance traveling-wave parametric amplifiers. Finally, we present a full design of an experiment to measure the predicted modification of the DOS by an embedded microwave field, within the reach of present-day technology.

ACKNOWLEDGMENTS

We are grateful to M. Skvortsov, K. Tikhonov, and P. J. de Visser for stimulating and helpful discussions. We acknowledge financial support from the Russian Science Foundation, Grant No. 17-72-30036.

-
- [1] A. Blais, R.-S. Huang, A. Wallraff, S. M. Girvin, and R. J. Schoelkopf, Cavity quantum electrodynamics for superconducting electrical circuits: An architecture for quantum computation, *Phys. Rev. A* **69**, 062320 (2004).
- [2] A. Wallraff, D. I. Schuster, A. Blais, L. Frunzio, R.-S. Huang, J. Majer, S. Kumar, S. M. Girvin, and R. J. Schoelkopf, Strong coupling of a single photon to a superconducting qubit using circuit quantum electrodynamics, *Nature* **431**, 162 (2004).
- [3] B. H. Eom, P. K. Day, H. G. LeDuc, and J. Zmuidzinas, A wideband, low-noise superconducting amplifier with high dynamic range, *Nat. Phys.* **8**, 623 (2012).
- [4] J. Zmuidzinas, Superconducting microresonators: Physics and applications, *Annu. Rev. Condens. Matter Phys.* **3**, 169 (2012).
- [5] P. J. de Visser, J. J. A. Baselmans, J. Bueno, N. Llombart, and T. M. Klapwijk, Fluctuations in the electron system of a superconductor exposed to a photon flux, *Nat. Commun.* **5**, 3130 (2014).
- [6] A. Moor, A. F. Volkov, and K. B. Efetov, Amplitude Higgs Mode and Admittance in Superconductors with a Moving Condensate, *Phys. Rev. Lett.* **118**, 047001 (2017).
- [7] R. Matsunaga, Y. I. Hamada, K. Makise, Y. Uzawa, H. Terai, Z. Wang, and R. Shimano, Higgs Amplitude Mode in the BCS Superconductors $\text{Nb}_{1-x}\text{Ti}_x\text{N}$ Induced by Terahertz Pulse Excitation, *Phys. Rev. Lett.* **111**, 057002 (2013).
- [8] R. Matsunaga, N. Tsuji, H. Fujita, A. Sugioka, K. Makise, Y. Uzawa, H. Terai, Z. Wang, H. Aoki, and R. Shimano, Light-induced collective pseudospin precession resonating with Higgs mode in a superconductor, *Science* **345**, 1145 (2014).
- [9] M. Beck, I. Rousseau, M. Klammer, P. Leiderer, M. Mitterdorff, S. Winnerl, M. Helm, G. N. Gol'tsman, and J. Demsar, Transient Increase of the Energy Gap of Superconducting NbN Thin Films Excited by Resonant Narrow-Band Terahertz Pulses, *Phys. Rev. Lett.* **110**, 267003 (2013).
- [10] M. Tinkham, *Introduction to Superconductivity* (Dover, New York, 2004).
- [11] S. M. Anlage, H. J. Snortland, and M. R. Beasley, A current controlled variable delay superconducting transmission line, *IEEE Trans. Magn.* **25**, 1388 (1989).
- [12] P. J. de Visser, D. J. Goldie, P. Diener, S. Withington, J. J. A. Baselmans, and T. M. Klapwijk, Evidence of a Nonequilibrium Distribution of Quasiparticles in the Microwave Response of a Superconducting Aluminum Resonator, *Phys. Rev. Lett.* **112**, 047004 (2014).
- [13] A. V. Semenov, I. A. Devyatov, P. J. de Visser, and T. M. Klapwijk, Coherent Excited States in Superconductors due to a Microwave Field, *Phys. Rev. Lett.* **117**, 047002 (2016).
- [14] J. Bardeen, Critical fields and currents in superconductors, *Rev. Mod. Phys.* **34**, 667 (1962).
- [15] M. Y. Kupriyanov and V. F. Lukichev, Temperature dependence of the critical depairing current in superconductors, *Fiz. Nizk. Temp.* **6**, 445 (1980) [*Sov. J. Low Temp. Phys.* **6**, 210 (1980)].
- [16] J. Romijn, T. M. Klapwijk, M. J. Renne, and J. E. Mooij, Critical pair-breaking current in superconducting aluminum strips far below T_c , *Phys. Rev. B* **26**, 3648 (1982).
- [17] A. Anthore, H. Pothier, and D. Esteve, Density of States in a Superconductor Carrying a Supercurrent, *Phys. Rev. Lett.* **90**, 127001 (2003).
- [18] M. Grifoni and P. Hänggi, Driven quantum tunneling, *Phys. Rep.* **304**, 229 (1998).
- [19] E. F. C. Driessen, P. C. J. J. Coumou, R. R. Tromp, P. J. de Visser, and T. M. Klapwijk, Strongly Disordered TiN and NbTiN s-Wave Superconductors Probed by Microwave Electrodynamics, *Phys. Rev. Lett.* **109**, 107003 (2012).
- [20] L. Grühaupt, M. Spiecker, D. Gusenkova, N. Maleeva, S. T. Skacel, I. Takmakov, F. Valenti, P. Winkel, H. Rotzinger, W. Wernsdorfer, A. V. Ustinov, and I. M. Pop, Granular aluminum as a superconducting material for high-impedance quantum circuits, *Nat. Mater.* **18**, 816 (2019).
- [21] A. I. Larkin and Y. N. Ovchinnikov, Nonlinear effects during vortex motion in superconductors, *Zh. Eksp. Teor. Fiz.* **73**, 299 (1977) [*Sov. Phys. JETP* **46**, 155 (1977)].
- [22] W. Belzig, F. K. Wilhelm, C. Bruder, G. Schön, and A. D. Zaikin, Quasiclassical Green's function approach to mesoscopic superconductivity, *Superlattices Microstruct.* **25**, 1251 (1999).
- [23] J. Rammer and H. Smith, Quantum field-theoretical methods in transport theory of metals, *Rev. Mod. Phys.* **58**, 323 (1986).
- [24] N. B. Kopnin, *Theory of Nonequilibrium Superconductivity* (Oxford University Press, Oxford, 2009).
- [25] K. D. Usadel, Generalized Diffusion Equation for Superconducting Alloys, *Phys. Rev. Lett.* **25**, 507 (1970).
- [26] T. H. Stoof and Yu. V. Nazarov, Kinetic-equation approach to diffusive superconducting hybrid devices, *Phys. Rev. B* **53**, 14496 (1996).
- [27] S. Guéron, Quasiparticles in a diffusive conductor: Interaction and pairing, Ph.D. thesis, Quantronics Group, CEA Saclay (1997).
- [28] We note a factor of 8 difference between our definition of α and the one used in Ref. [31]. We also point out that there is a misprint, an omitted factor of 1/4, in the definition of α in Ref. [13].
- [29] The condition for the “quantum mode of depairing” $\alpha/\Delta \ll \hbar\omega_0/\Delta$ can be rewritten as $\langle I_{rf}^2 \rangle / I_c^2 \ll 0.028\hbar\omega_0/\Delta$, where $\langle I_{rf}^2 \rangle$ is the mean-square amplitude of the induced rf current and I_c is the depairing current.
- [30] N. B. Kopnin and A. S. Melnikov, Proximity-induced superconductivity in two-dimensional electronic systems, *Phys. Rev. B* **84**, 064524 (2011).
- [31] K. S. Tikhonov, M. A. Skvortsov, and T. M. Klapwijk, Superconductivity in the presence of microwaves: Full phase diagram, *Phys. Rev. B* **97**, 184516 (2018).
- [32] A. V. Semenov, I. A. Devyatov, and M. Y. Kupriyanov, Theoretical analysis of the operation of the kinetic

- inductance-based superconducting microwave detector, *JETP Lett.* **88**, 441 (2008).
- [33] I. Snyman and Yu. V. Nazarov, Bistability in voltage-biased normal-metal/insulator/superconductor/insulator/normal-metal structures, *Phys. Rev. B* **79**, 014510 (2009).
- [34] P. K. Tien and J. P. Gordon, Multiphoton process observed in the interaction of microwave fields with the tunneling between superconductor films, *Phys. Rev.* **129**, 647 (1963).
- [35] T. Kommers and J. Clarke, Measurement of Microwave-Enhanced Energy Gap in Superconducting Aluminum by Tunneling, *Phys. Rev. Lett.* **38**, 1091 (1977).
- [36] R. Horstman and J. Wolter, Gap enhancement in narrow superconducting tunneljunctions induced by homogeneous microwave currents, *Phys. Lett. A* **82**, 43 (1981).
- [37] J. Wolter and R. Horstman, Determination of the quasiparticle energy distribution in superconducting tunnel junctions under microwave irradiation, *Phys. Lett. A* **86**, 185 (1981).
- [38] G. R. Boogaard, A. H. Verbruggen, W. Belzig, and T. M. Klapwijk, Resistance of superconducting nanowires connected to normal-metal leads, *Phys. Rev. B* **69**, 220503(R) (2004).
- [39] <http://www.cst.de>.
- [40] D. C. Mattis and J. Bardeen, Theory of the anomalous skin effect in normal and superconducting metals, *Phys. Rev.* **111**, 412 (1958).
- [41] G. Catelani, L. I. Glazman, and K. E. Nagaev, Effect of quasiparticles injection on the ac response of a superconductor, *Phys. Rev. B* **82**, 134502 (2010).
- [42] S. Chaudhuri, D. Li, K. D. Irwin, C. Bockstiegel, J. Hubmayr, J. N. Ullom, M. R. Vissers, and J. Gao, Broadband parametric amplifiers based on nonlinear kinetic inductance artificial transmission lines, *Appl. Phys. Lett.* **110**, 152601 (2017).
- [43] A. A. Adamyan, S. E. de Graaf, S. E. Kubatkin, and A. V. Danilov, Superconducting microwave parametric amplifier based on a quasi-fractal slow propagation line, *J. Appl. Phys.* **119**, 083901 (2016).